Carbohydrate Polymers 102 (2014) 862–868

Contents lists available at ScienceDirect

Carbohydrate Polymers

journal homepage: www.elsevier.com/locate/carbpol

In situ forming spruce xylan-based hydrogel for cell immobilization

Volodymyr Kuzmenko[a,b], Daniel Hägg[c], Guillermo Toriz[a,d], Paul Gatenholm[a,c,*]

[a] Wallenberg Wood Science Center, Kemivägen 4, SE-412 96 Gothenburg, Sweden
[b] Department of Microtechnology and Nanoscience, Chalmers University of Technology, Kemivägen 9, SE-412 96 Gothenburg, Sweden
[c] Department of Chemical and Biological Engineering, Chalmers University of Technology, Kemivägen 4, SE-412 96 Gothenburg, Sweden
[d] Department of Wood, Cellulose and Paper Research, University of Guadalajara, Juárez 976, 44100 Guadalajara, Mexico

ARTICLE INFO

Article history:
Received 15 August 2013
Received in revised form 9 October 2013
Accepted 27 October 2013
Available online 4 November 2013

Keywords:
Hydrogel
Xylan
Conjugate
Enzymatic crosslinking
Cell immobilization

ABSTRACT

An *in situ* forming spruce xylan-based hydrogel was synthesized in two steps with the intended use of cell encapsulation and *in vivo* delivery. First, bioconjugate was obtained through the reaction of glucuronic acid groups from xylan backbone with tyramine (TA). After that, the gelation process was enabled by enzymatic crosslinking of the phenol-containing TA-xylan conjugate. Exhibiting an exponential increase in the storage modulus, a 3D gel network was formed in about 20 s. The designed gel showed extensive swelling and retained its mechanical integrity for more than two months. Mesenchymal stem cells were encapsulated in the hydrogel and cultured for one week. The cells retained their adipogenic differentiation capacity inside the gel, as verified by lipid accumulation. From these facts, we conclude that spruce xylan is a promising precursor for *in situ* forming hydrogels and should be evaluated further for tissue engineering purposes.

1. Introduction

Hydrogels have been continuously attracting attention of biochemical engineers in the field of cell delivery (Jin et al., 2011; Liu & Chan-Park, 2010; Plunkett & Hailey, 1990; Stafford et al., 1992) since crosslinked HEMA hydrogel for contact lenses was created in 1960 (Wichterle & Lim, 1960). The reason is that hydrogels can meet therapeutic or tissue engineering needs as suitable extracellular matrices (ECMs) (Kretlow, Klouda, & Mikos, 2007). For successful immobilization of cells, hydrogels must be biocompatible (Anderson, 1988), have high water absorption while keeping their chemical and mechanical stability (Lindblad, Albertsson, Ranucci, Laus, & Giani, 2005), provide sufficient diffusion of necessary nutrients for cells and waste metabolites, be able to guide attachment and differentiation of the encapsulated cells, protect cells from mechanical stresses during their integrity into new tissue, and isolate cells from body immune response (Jen, Wake, & Mikos, 1996). Recently, *in situ* forming, injectable hydrogels have started to dominate in biomedical applications over traditional preformed hydrogels as they can be inserted into the target region by straight injection with minimal invasive damage, providing homogeneous distribution of bioactive molecules in the surrounding tissue (Kretlow et al., 2007; Van Tomme, Storm, & Hennink, 2008).

Hemicellulose (HC) as a raw material for production of hydrogels has several useful characteristics: biocompatibility, biodegradability, non-toxicity, and abundance (Ebringerova, Hromadkova, & Heinze, 2005; Edlund & Albertsson, 2008). In comparison to hyaluronan (Dahl, Dahl, Enstrom-Laurent, & Granath, 1985), alginate (Lee et al., 2007) and chitosan (Kim, Seo, Moon, Yoo, & Park, 2008), which are the polysaccharides commonly used to produce hydrogels for tissue engineering or drug delivery (Barbucci, 2009), HC from wood have much higher resource potential and result in less biodegradable products. In fact, HC are the third most plentiful polymers in lignocellulosic biomass after cellulose and lignin (Gatenholm & Tenkanen, 2004). The presence of hydroxyl and carboxylic groups on the HC chains makes them suitable for chemical or enzymatic modifications while keeping their morphology and native structure. In previous studies this feature has been used to introduce functional groups onto HC structure and subsequently obtain crosslinked HC-based hydrogels for various biomedical applications (Albertsson, Voepel, Edlund, Dahlman, & Söderqvist-Lindblad, 2010; Edlund & Albertsson, 2008; Karaaslan, Tshabalala, Yelle, & Buschle-Diller, 2011; Sun, Wang, Jing, & Mohanathas, 2013; Yang, Zhou, & Fang, 2011), however none of those hydrogels was characterized by fast gelation time in the range of 1 min.

Spruce xylan is a natural, biodegradable polysaccharide that is composed of arabinose, 4-O-methyl-glucuronic acid (10 wt%) and

Abbreviations: TA, tyramine; ECM, extracellular matrix; MSCs, mesenchymal stem cells; HRP, horseradish peroxidase; NHS, N-hydroxysuccinimide; EDAC, N-ethyl-N′-(3-dimethylaminopropyl) carbodiimide hydroxide; PBS, phosphate buffered saline; BME, basal medium Eagle.

* Corresponding author at: Wallenberg Wood Science Center, Kemivägen 4, SE-412 96 Gothenburg, Sweden. Tel.: +46 031 772 34 07; fax: +46 031 772 34 18.
E-mail addresses: kuzmenko@chalmers.se (V. Kuzmenko), daniel.hagg@chalmers.se (D. Hägg), guillert@chalmers.se (G. Toriz), paul.gatenholm@chalmers.se (P. Gatenholm).

0144-8617/$ – see front matter © 2013 Elsevier Ltd. All rights reserved.
http://dx.doi.org/10.1016/j.carbpol.2013.10.077

xylose in a ratio of 1:2:11 respectively (Escalante et al., 2012). Contrary to other (1–4)-glycosidic-linked polysaccharides, xylans do not have reduced water solubility due to their low molecular weight and high degree of side chain substitution (Ebringerova & Heinze, 2000). As a result, crosslinking is necessary to form hydrogel network from hydrophilic xylan polymer (Chimphango, van Zyl, & Görgens, 2012). Carboxylic groups present in glucuronic acid residues can be utilized to produce functionalized conjugates for succeeding crosslinking (Gabrielii & Gatenholm, 1998; Gabrielii, Gatenholm, Glasser, Jain, & Kenne, 2000).

A mechanism of gelation plays an important role in defining the properties of hydrogels. Enzymatic crosslinking is viewed as a very convenient method for fabrication of *in situ* forming chemically crosslinked hydrogels that can be used in biological systems. Many different enzymes have been evaluated in this research field, depending on the functionality of the initial materials (Johnson, Fairbanks, Anseth, & Bowman, 2009; Sperinde & Griffith, 1997; Toledano, Williams, Jayawarna, & Ulijn, 2006; Westhaus & Messersmith, 2001). Horseradish peroxidase (HRP) was successfully used to fabricate injectable hydrogels for both tissue engineering and drug delivery applications. This enzyme catalyzes the coupling of phenol or aniline derivatives *via* decomposition of hydrogen peroxide (H_2O_2) (Kobayashi, Uyama, & Kimura, 2001). Previously, precursor macromolecules functionalized with tyramine (TA) side groups were crosslinked with a combination of HRP and H_2O_2 and the resulting hydrogels were reported to be innocuous, have sufficient mechanical properties and short gelation times at certain pH and concentrations of HRP and H_2O_2 (Jin, Hiemstra, Zhong, & Feijen, 2007; Lee, Chung, & Kurisawa, 2009; Sakai, Hirose, Taguchi, Ogushi, & Kawakami, 2009).

In this research, the novel *in situ* forming injectable hydrogel from spruce xylan is described. The gelation is based on enzymatic crosslinking of xylan-TA conjugate using HRP and H_2O_2. Xylan-based hydrogel is evaluated for its cell immobilization capability as ECM.

2. Experimental

2.1. Materials

Xylan (Mw = 12,700, 10 wt% of 4-O-methyl-glucuronic acid units) was extracted from spruce as previously reported by Escalante et al. (2012). In brief, hollocellulose was obtained from spruce wood by extensive delignification with acidic sodium chlorite over 60 h at 70–80 °C. The hollocellulose was further treated with 24 wt% KOH, and galactoglucomannans were precipitated with $Ba(OH)_2$. The supernatant was then treated with acidic ethanol (supernatant:EtOH 96%:glacial CH_3COOH in the ratio 1:4:0.4 v:v:v respectively) to precipitate arabinoglucuronoxylan. N-hydroxysuccinimide (NHS), N-ethyl-N′-(3-dimethylaminopropyl) carbodiimide hydroxide (EDAC), TA, HRP (260 purpurogallin unit/mg solid), anhydrous N,N-dimethylformamide (DMF), and deuterium oxide (D_2O) were purchased from Sigma–Aldrich (USA) and used without further purification. H_2O_2 was obtained from Riedel-de-Häen (Germany). Mouse mesenchymal stem cells (MSCs, line C3H10T1/2) were purchased from ATCC (USA) and cultured in Basal Medium Eagle (BME) or adipogenic differentiation medium (Dulbecco's modified eagle medium, 10% fetal bovine serum, 1% antibiotics/antimycotic, 0.5 mM 3-isobutyl-1-methylxanthine, 60 μl indomethacin, 1 μl dexamethasone, 2 μl insulin) from HyClone (USA). Dulbecco's phosphate buffered saline solution (PBS 1×, without Ca & Mg) was purchased from PAA Laboratories (Austria). MilliQ water used in all phases of the experiment was deionized and further purified with Millipore Synergy UV unit.

2.2. Methods

2.2.1. Synthesis of xylan-TA conjugate

Xylan-TA conjugate was synthesized by the coupling reaction of primary amine groups from TA to carboxylic groups from glucuronic acid units in xylan. Xylan (0.5 g, 0.306 mmol COOH) was first dissolved in 20 ml H_2O after stirring and slight heating for 30 min. An EDAC/NHS mixture was then added to the xylan solution for activation of carboxylic groups, and the solution was stirred for 30 min. After that, 62.3 mg of TA was dissolved in 6 ml DMF (the molar ratio for EDAC/NHS/COOH was 1.8/1.8/1, for TA/COOH – 1.5/1). This solution was slowly added to the reaction flask with xylan to avoid precipitation of xylan in DMF. The mixture was left stirring at room temperature under N_2 for 3 days. The formed xylan-TA conjugate was precipitated in cold ethanol, collected on a ceramic filter during vacuum filtration and dried in a vacuum oven. The yield was 0.4 g (80%). The composition was defined by ^{1}H NMR and by FTIR spectroscopy.

2.2.2. Hydrogel formation

Hydrogel samples (0.5 ml) were prepared in vials at room temperature. The concentration of the conjugate in hydrogels was about 5 wt%. First, conjugate was dissolved in PBS (25 mg in 350 μl) after stirring for 20 min. Following this, a PBS solution of H_2O_2 (52 μl of 0.3 wt% stock solution, about 90 mM) and HRP (48 μl of 0.6 mg/ml stock solution) was added and the mixture was gently shaken. The H_2O_2/TA molar ratio used in the experiment was 0.15 mol/mol, and the HRP/TA ratio was 0.5 mg/mmol. The gelation time was established by the vial tilting method, *i.e.* no flow within 1 min after inverting the vial was regarded as the gel state.

2.2.3. Expansion of MSCs

C3H10T1/2 cells were removed from liquid N_2, thawed and transferred to a 75-cm^2 cell culture flask containing 12 ml of BME. The cell culture flask was placed in an incubator (37 °C, 5% CO_2, 95% relative humidity). The medium was changed every three to four days and the cells were passaged when 80% confluence was reached.

2.2.4. Cell entrapment

The conjugate was dissolved in 400 μl of cell suspension at a cell density of 5×10^6 cells/ml. The solution was then divided into eight parts, and each was mixed with HRP and H_2O_2 stock solutions (6 μl of both) to form hydrogel with immobilized cells. The final concentration of conjugate in the hydrogels was 5 wt%. The whole procedure was performed under sterile conditions; reagents were sterilized by filtration through 0.22-μm pore size filters.

2.2.5. Cell differentiation

1 ml of BME was added to each sample after 10 min of gelation. The immobilized hydrogels were placed in an incubator; this was denoted day 0. The media were changed every three to four days, and samples were taken at day 7.

For microscopy analyses (SEM and confocal), 70 mg/ml TA-conjugate was dissolved in a cell suspension with 6.25×10^6 cells/ml. After that, 40 μl droplets were pipetted into 24-well plates, and each droplet was mixed with 5 μl of HRP (0.6 mg/ml) and 5 μl of 0.3% H_2O_2 to form a hydrogel with immobilized cells. The final cell concentration in the hydrogels was 5×10^6 cells/ml. The whole procedure was performed under sterile conditions; reagents were sterilized by filtration through 0.22-μm pore size filters.

2.2.6. Confocal microscopy

The cells were stained by adding 0.5 ml of non-complete BME with 1 mM Celltracker Red CMTPX, 1 drop of Hoechst 33342

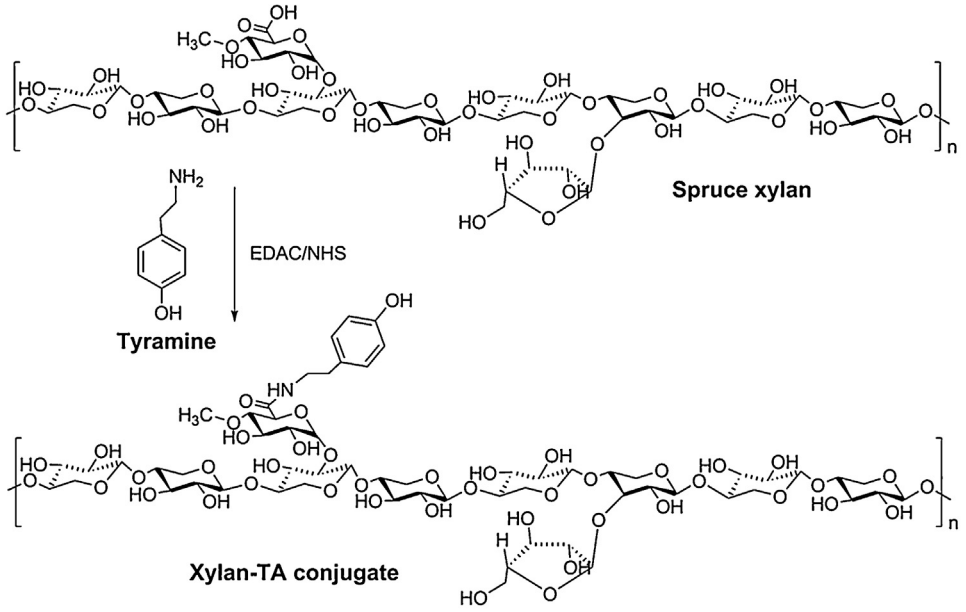

Fig. 1. Chemical reaction of conjugate formation from spruce xylan and tyramine.

ready-to-use and 0.75 μg Bodipy (all from Invitrogen) to each well and incubated for 30 min. The staining solution was then replaced with 0.5 ml of complete BME and incubated for another 30 min. The samples were thereafter fixated in 4% formaldehyde and stored in PBS until visualization.

2.2.7. Scanning electron microscopy

For SEM analysis, the hydrogel was dehydrated in baths of increasing ethanol concentrations (70%, 80%, 90% and 95%). The samples were put in t-butanol, frozen at 4 °C, placed in a −80 °C freezer and freeze dried in a lyophilizer (Heto, PowerDry, PL3000). The samples were positioned on SEM stubs with adhesive tape (TAAB) and sputter coated for 1 min (Sputter Coater s150B, Edwards) with a thin gold layer. SEM analysis was performed with a Leo Ultra 55 FEG-SEM.

Before immersion in ethanol, the hydrogels with immobilized cells were washed two times in PBS to remove media residues and fixated for 2 h in 2.5% glutaraldehyde in PBS. The glutaraldehyde was removed by rinsing the samples two times in PBS.

2.2.8. ^1H NMR

^{1}H NMR (400 MHz) spectra were recorded on a Varian-Agilent spectrometer. Conjugate was dissolved in D_2O at a concentration of 0.015 g/ml. The degree of TA substitution was evaluated as the ratio between glucuronic acid units conjugated with TA and the total amount of acidic units in the initial spruce xylan. It was quantitatively measured by integral calculation of the signals given by aromatic (δ 6.75 and 7.05) and anomeric protons (δ 5.15–5.30).

2.2.9. FTIR spectroscopy

Experimental solid samples for FTIR spectra were obtained by making 100-mg pellets with a ratio of KBr/sample = 99/1. FTIR spectroscopic analysis (Perkin Elmer FTIR 2000) was set on transmission mode; the wavenumber range was between 4000 and 370 cm^{-1}.

2.2.10. Degree of swelling

After lyophilization, the dry hydrogels (W_d) were immersed in 3 ml of PBS at 37 °C for 2 days in order to reach the swelling equilibrium. Swollen samples were first removed from PBS and, after removal of surface water, were weighed (W_s). The degree of swelling of the hydrogel was calculated as follows: $(W_s - W_d)/W_d$.

2.2.11. Rheological analysis

The rheology of the gel formation was monitored at 37 °C in a Bohlin CS Rheometer (in oscillatory mode, parallel plate configuration) by applying a constant shear stress of 2 Pa at a frequency of 1 Hz. Under these conditions the shear strain was in the vicinity of 5% within the first few seconds; after that it decreased to values lower than 1% in 30 s and for most of the monitored time the shear strain remained at the values lower than 0.1% (*i.e.* in the linear viscoelastic region). 400 μl solution of conjugate in PBS was carefully placed in the lower plate and 52 μl of peroxide was then added (0.3% solution in PBS). Gelation started after addition of 48 μl of HRP (0.6 mg/ml of PBS) to the sample; the upper plate was set in position (0.5 mm gap). The measurements of storage and loss moduli were documented as a function of time every 5 s for 10 min. Three samples were prepared for the rheological analysis.

3. Results and discussion

3.1. Xylan-TA conjugate

Chemical interaction between the EDAC/NHS-activated carboxylic groups present in spruce xylan and the excess amount of amine groups of TA resulted in the formation of the xylan-TA conjugate *via* amide bonds, as shown in Fig. 1.

^{1}H NMR was used to confirm the presence of the conjugate after reaction and to determine the degree of TA substitution. The peaks assigned for xylan anomeric protons (I, δ 5.15–5.30) and xylose unit protons (II, δ 3.10–4.60) were present in both spectra (*i.e.* initial xylan and the synthesized conjugate product) since the xylan backbone remained untouched (Fig. 2A and B). The success of the reaction was confirmed by the appearance of the new peaks corresponding to aromatic protons (III, δ 6.75 and 7.05) and methylene protons (IV, δ 2.65–2.75) from TA (Fig. 2B). The quantitative analysis of ^{1}H NMR showed about 76% of TA substitution.

FTIR spectroscopy was used to analyze the changes in the chemical structure after the amidation reaction between glucuronic acid unit of xylan and tyramine (Fig. 3). The strongest absorption bands

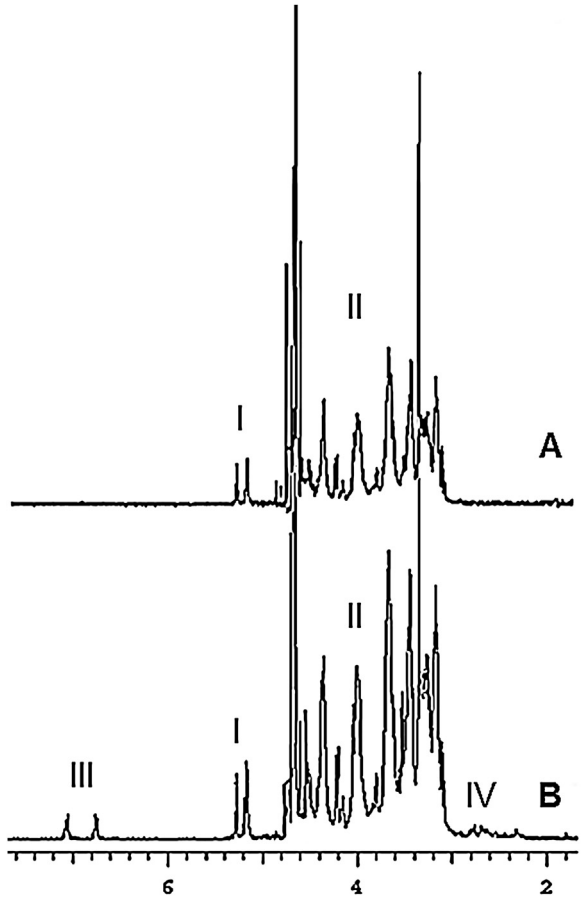

Fig. 2. ^{1}H NMR spectra. (A) Initial xylan, (B) Xylan-TA conjugate. I – xylan anomeric protons, II – xylose unit protons, III – TA aromatic protons, IV – TA methylene protons.

in the IR spectra of the analyzed spruce xylan and xylan-based conjugate were observed at around 3700–3000 and 1200–1000 cm^{-1} corresponding to CO—H stretching vibrations with a maximum at 3410 cm^{-1} and C—OH stretching vibrations with a maximum at 1042 cm^{-1}. The other main adsorption bands of the FTIR spectrum of xylan were represented by stretching vibrations of CH_3, CH_2 and CH groups in the frequency range of 3050–2800 cm^{-1}, COO— bands

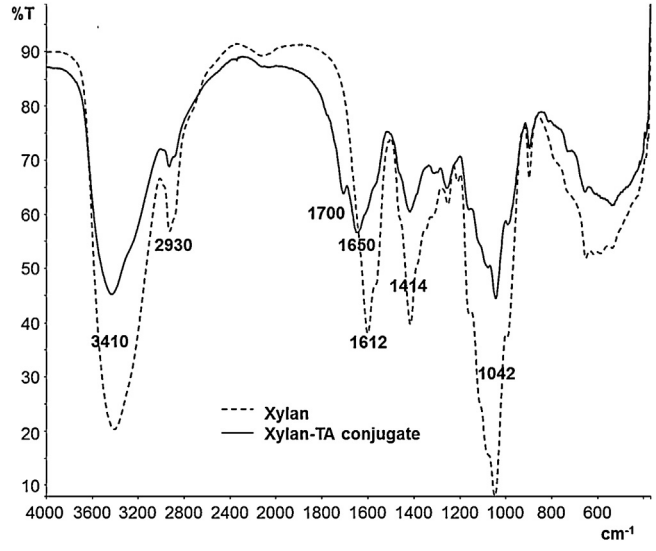

Fig. 3. FTIR spectrum of conjugate in comparison to initial xylan.

with a maximum intensity at 1612 and 1414 cm^{-1}, and C—C from xylopyranose units in the region of 1300–800 cm^{-1} (Buslov et al., 2009). The appearance of COO— groups in the spectra indicated the presence of glucuronic acid units in the chemical structure of the spruce xylan. In contrast, FTIR spectra of the synthesized conjugate had characteristic peaks represented by stretching vibrations of the TA substituent at around 1700 cm^{-1} (aromatic C=C) and 1650 cm^{-1} (C=O in amide bond), while carboxylate peaks of initial xylan disappeared or decreased significantly. Thus, FTIR spectroscopy also confirmed the fact of conjugate production.

3.2. In situ forming hydrogel

The formation of hydrogel took place when the HRP/H_2O_2 combination was added (Fig. 4). During and after addition of HRP/H_2O_2, the mixture was gently shaken in order to avoid formation of high crosslinking density regions (clusters) dispersed within regions of low crosslinking density and to achieve a homogenous structure of hydrogel at the end.

The crosslinking of phenol-containing xylan-TA conjugates can occur *via* the appearance of two possible types of bonds: (1) C—C bonds between two carbon atoms at the ortho positions; (2) C—O bonds between the carbon atom at the ortho position and the oxygen atom from the phenolic group (Fukuoka, Uyama, & Kobayashi, 2005).

The polymer concentration and ratios between reagents (HRP/TA and H_2O_2/TA) have a large impact on gelation time. Jin et al. (2007) previously investigated this influence on the formation of dextran-TA hydrogels and optimized the conditions of crosslinking a conjugated polysaccharide with HRP/H_2O_2. In this study, the lower concentrations of peroxide were used in order to avoid cytotoxicity problems that H_2O_2 may cause. Previous *in vivo* studies showed that hydrogels crosslinked in the presence of 100 mM H_2O_2 are biocompatible and non-toxic (Jin, Moreira Teixeira, Dijkstra, Zhong, et al., 2010; Kurisawa, Chung, Yang, Gao, & Uyama, 2005).

Using the tilting method the average time of gelation was measured to be about 20 s (20 ± 5 s), which is very good for *in situ* forming hydrogels. Fast gel formation keeps the gel shape intact inside the body, thus preventing diffusion of active substances outside the gel. The enzymatic crosslinking of xylan-containing conjugates enabled comparatively rapid gelation in comparison with previously reported *in situ* forming hydrogels from HC (Edlund & Albertsson, 2008; Lindblad et al., 2005; Yang et al., 2011).

3.3. Degree of swelling

The fact that hydrogels are able to retain considerable amounts of water without disintegration makes them suitable material for cell encapsulation with subsequent delivery to a living organism. In our study, xylan-based hydrogel was able to swell up to 14 times its dry weight after 2 days of immersion in PBS until it reached its equilibrium swelling level. Such a high degree of swelling of hydrogels can be explained by the low crosslinking density of xylan-TA conjugate due to the relatively low amount of glucuronic acid units in the spruce xylan chemical structure. However, no structural disintegration of the swollen hydrogel was observed thereafter for several months. The sufficient amount of water in a hydrogel (especially free water) is important, as is the porous network, since both factors determine the absorption and diffusion of necessary nutrients for cells through the hydrogel. Furthermore, an aqueous environment protects cells from a potential immune response (Hoffman, 2002).

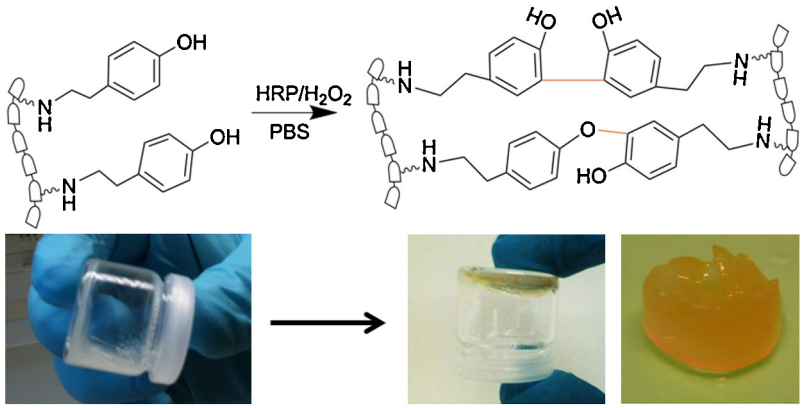

Fig. 4. Chemical reaction of enzymatic crosslinking of xylan-TA conjugates (top); illustration of gel formation established by the tilting method (bottom).

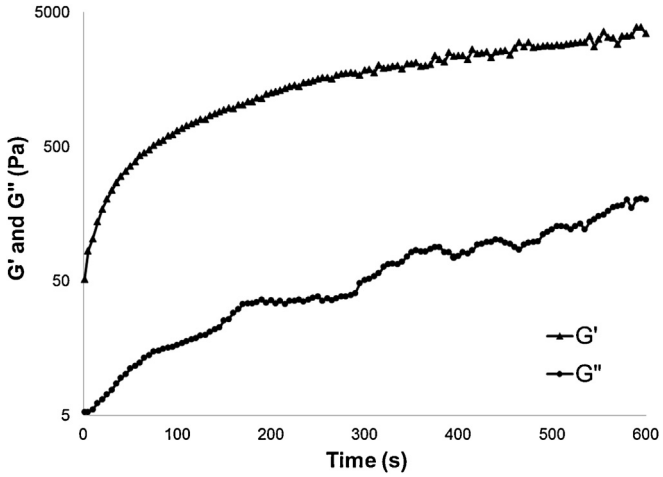

Fig. 5. Rheology of gel formation from xylan-TA conjugate as a function of time.

3.4. Rheological analysis

The mechanical properties of the xylan-based hydrogels were studied by oscillatory rheology experiments on *in situ* forming gels prepared as mentioned above. The storage modulus (G') and loss modulus (G'') were recorded in time to study the kinetics of hydrogel formation. Fig. 5 shows the *in situ* gelation process of xylan-TA conjugate (5 wt% concentrations) as it took place in the rheometer. It can be seen that, in this system, gelation occurred almost instantly. The storage modulus increased exponentially (two orders of magnitude) in the first 15–25 s, which suggests the formation of a 3D network. These results correlate with the gelation time measured by the simple tilting method. Furthermore, the storage modulus (G') for the samples tested was always larger than the loss modulus (G''), indicating elastic behavior and confirming that crosslinking of the material occurred in the very first stages of gelation. Rheological monitoring of gelation for other polymeric systems has shown that, when the storage modulus is lower than the loss modulus, the system behaves mainly as a solution and only after a gelation point has been achieved, elastic phenomena would dominate (Weng, Chen, & Chen, 2007).

In order to be efficient ECM for temporary support for cells, hydrogels have to withstand biomechanical loading without excessive deformation. Depending on the mechanical properties of particular natural tissue, the hydrogels must have a satisfactory storage modulus. Chemically crosslinked hydrogels must be mechanically strong enough to be suitable for tissue engineering applications (Jin, Moreira Teixeira, Dijkstra, Zhong, et al., 2010). The storage moduli (G') of the xylan-TA hydrogels after gelation was in the range of 1–4 kPa, which is comparable with the previously reported enzymatically crosslinked hydrogels (Jin, Moreira Teixeira, Dijkstra, van Blitterswijk, et al., 2010; Lee, Chung, & Kurisawa, 2008) and can be viewed as an appropriate material for ECM.

3.5. Morphology

The morphology of lyophilized hydrogels was analyzed using SEM (Fig. 6). The hydrogel porosity needs to be sufficient to allow fast diffusion of nutrients for cells to grow and proliferate. The xylan-TA hydrogels were highly porous with a well-interconnected pore structure. They were characterized by a wide pore size distribution; the estimated pore size was in the range of 2–20 μm. In further cell studies, it will be shown that the hydrogel porosity is satisfactory for cell immobilization.

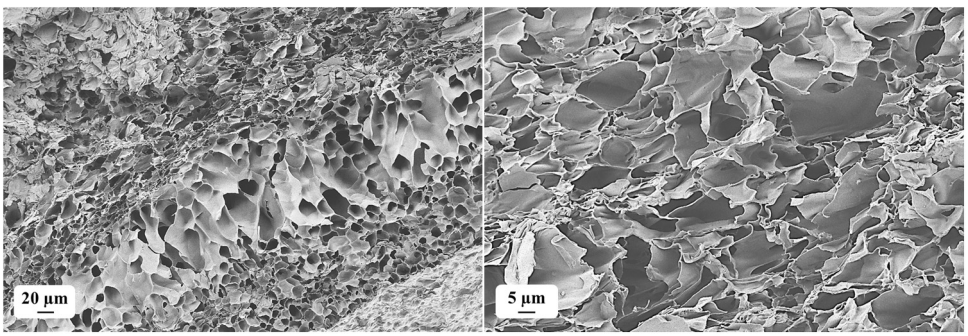

Fig. 6. SEM images of lyophilized hydrogel samples (left-mag = 500×, right-mag = 2k×).

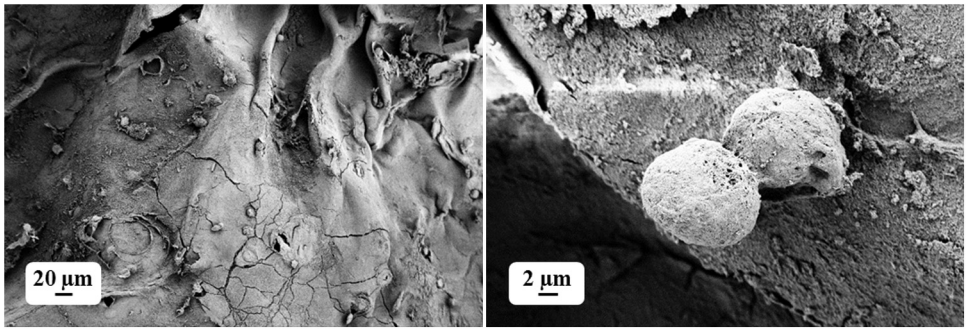

Fig. 7. SEM images of C3H10T1/2 cells encapsulated in the TA-hydrogel and cultured for seven days, showing the distribution of cells on the surface of the TA-hydrogel after lyophilization (left-mag = 500×, right-mag = 5k×).

3.6. Cell differentiation

Both SEM and confocal microscopy verified the distribution of cells in the TA-hydrogel, however rather scarcely distributed. The SEM images, Fig. 7, showed the presence of cells on the surface of the freeze-dried hydrogel. In the higher magnification, as seen on the right-hand side, a round shape can be seen that is typical for cell differentiation. The confocal microscopy, Fig. 8, showed cells cultured in adipogenic differentiation medium displaying an adipocyte morphology with lipid droplet accumulation (B1&2) as compared to control cells grown in regular growth medium, which showed very little lipid accumulation (A1&2). Red indicates cytoplasm, blue indicates nuclei and green indicates lipids.

The results confirmed that the cells can actually be differentiated toward adipocytes inside the gel, as indicated by the lipid droplet formation, a hallmark of adipocyte formation. This suggests that the TA-hydrogel/cell combination may have the potential to be used as an injectable filler material when correcting small cavity defects or for cosmetic purposes, which is usually performed using synthetic materials or autologous tissue (Garfein, Orgill, & Pribaz, 2003). Problems with the former method include rupture and dislocation and with the latter, there may be problems such as volume retention, cyst formation and local necrosis (Bauer-Kreisel, Goepferich, & Blunk, 2010). The use of the patient's own cells and finding a way to integrate them where needed could be a potential way to increase surgical success. This type of reconstructive surgery, tissue engineering, is largely considered to be the future in regenerative medicine, where stem cells or other cells in combination with an automatic machine are used to repair damaged or diseased tissue (Polak & Bishop, 2006). Potentially, the TA-hydrogel could also be used for delivery of other cell types for *in vivo* studies and for setting up a 3D environment for *in vitro* cell studies. These

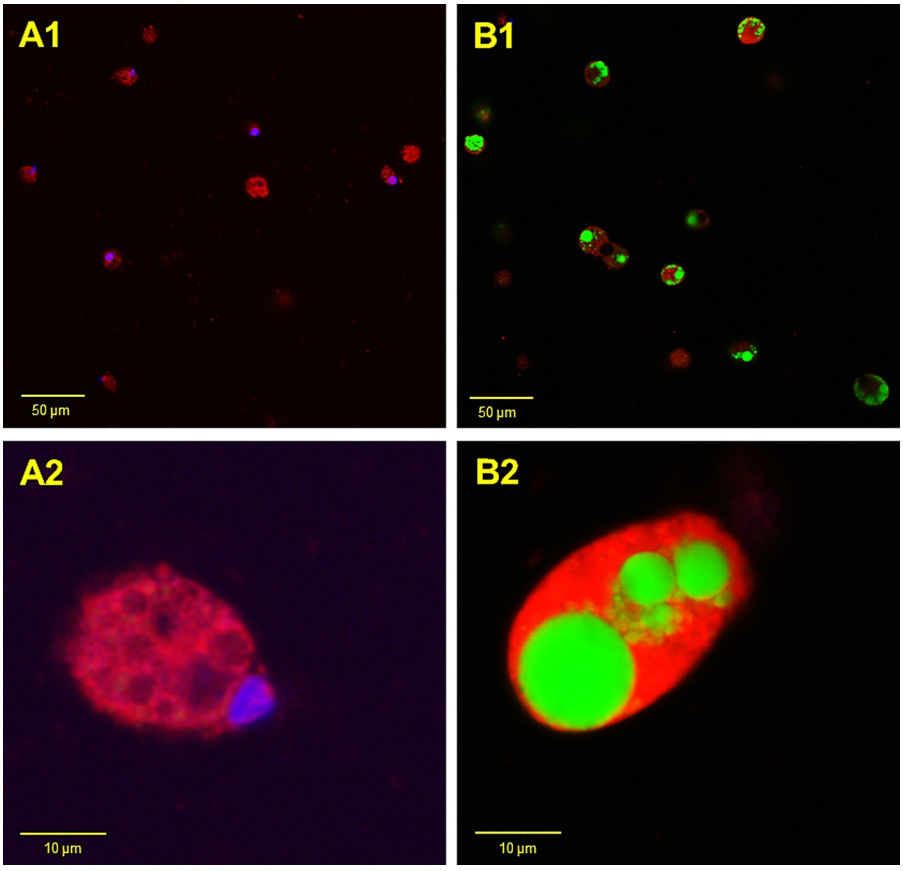

Fig. 8. Confocal images of cells encapsulated in TA-hydrogel after seven days of culture.

are generally considered to provide more reliable results than conventional 2D cell cultures with respect to screening drugs targeting for instance the metabolic syndrome (Xu, Wang, Yan, Yao, & Ge, 2010).

4. Conclusions

Xylan isolated from spruce has been successfully conjugated with tyramine using EDAC/NHS activation of glucuronic acid in spruce arabinoglucuronoxylan. This conjugate was enzymatically crosslinked with HRP to provide gelation within 20 ± 5 s at room temperature, which is the best result achieved for any HC-based hydrogel so far. Hydrogels showed mechanical integrity and an interconnected porous structure, as well as high degree of swelling. This system was used for *in situ* immobilized mesenchymal stem cells, and the cells were able to differentiate into adipocytes, as shown by SEM and confocal microscopy.

We conclude that the spruce xylan-based hydrogel can be used to encapsulate mesenchymal stem cells and that the cells retain their ability to differentiate toward adipocytes, which may be further evaluated for tissue engineering purposes.

Acknowledgements

The Wallenberg Wood Science Center funded by the Knut and Alice Wallenberg Foundation is greatly acknowledged for their financial support. We also thank Bengt Hagström for his assistance with rheological analysis.

References

Albertsson, A.-C., Voepel, J., Edlund, U., Dahlman, O., & Söderqvist-Lindblad, M. (2010). Design of renewable hydrogel release systems from fiberboard mill wastewater. *Biomacromolecules*, *11*, 1406–1411.

Anderson, J. M. (1988). Inflammatory response to implants. *Transactions – American Society for Artificial Internal Organs*, *34*, 101–107.

Barbucci, R. (2009). *Hydrogels: Biological properties and applications*. Milan: Springer-Verlag Italia.

Bauer-Kreisel, P., Goepferich, A., & Blunk, T. (2010). Cell-delivery therapeutics for adipose tissue regeneration. *Advanced Drug Delivery Reviews*, *62*, 798–813.

Buslov, D. K., Kaputski, F. N., Sushko, N. I., Torgashev, V. I., Solov'eva, L. V., Tsarenkov, V. M., et al. (2009). Infrared spectroscopic analysis of the structure of xylans. *Journal of Applied Spectroscopy*, *76*, 801–805.

Chimphango, A. F. A., van Zyl, W. H., & Görgens, J. F. (2012). *In situ* enzymatic aided formation of xylan hydrogels and encapsulation of horse radish peroxidase for slow release. *Carbohydrate Polymers*, *88*, 1109–1117.

Dahl, L. B., Dahl, I. M., Enstrom-Laurent, A., & Granath, K. (1985). Concentration and molecular weight of sodium hyaluronate in synovial fluid from patients with rheumatoid arthritis and other arthropathies. *Annals of the Rheumatic Diseases*, *44*, 817–822.

Ebringerova, A., & Heinze, T. (2000). Xylan and xylan derivatives – Biopolymers with valuable properties, 1 – Naturally occurring xylans structures, procedures and properties. *Macromolecular Rapid Communications*, *21*, 542–556.

Ebringerova, A., Hromadkova, Z., & Heinze, T. (2005). Hemicellulose. *Advances in Polymer Science*, *186*, 1–67.

Edlund, U., & Albertsson, A.-C. (2008). A microspheric system: Hemicellulose-based hydrogels. *Journal of Bioactive and Compatible Polymers*, *23*, 171–186.

Escalante, A., Gonçalves, A., Bodin, A., Stepan, A., Sandström, C., Toriz, G., et al. (2012). Flexible oxygen barrier films from spruce xylan. *Carbohydrate Polymers*, *87*, 2381–2387.

Fukuoka, T., Uyama, H., & Kobayashi, S. (2005). Polymerization of polyfunctional macromolecules: Synthesis of a new class of high molecular weight poly(amino acid)s by oxidative coupling of phenol-containing precursor polymers. *Biomacromolecules*, *5*, 977–983.

Gabrielii, I., & Gatenholm, P. (1998). Preparation and properties of hydrogels based on hemicellulose. *Journal of Applied Polymer Science*, *69*, 1661–1667.

Gabrielii, I., Gatenholm, P., Glasser, W. G., Jain, R. K., & Kenne, L. (2000). Separation, characterization and hydrogel-formation of hemicellulose from aspen wood. *Carbohydrate Polymers*, *43*, 367–374.

Garfein, E. S., Orgill, D. P., & Pribaz, J. J. (2003). Clinical applications of tissue engineered constructs. *Clinics in Plastic Surgery*, *30*, 485–498.

Gatenholm, P., & Tenkanen, M. (2004). *Hemicelluloses: Science and technology*. New York: Oxford University Press.

Hoffman, A. S. (2002). Hydrogels for biomedical applications. *Advanced Drug Delivery Reviews*, *43*, 3–12.

Jen, A. C., Wake, M. C., & Mikos, A. G. (1996). Review: Hydrogels for cell immobilization. *Biotechnology and Bioengineering*, *50*, 357–364.

Jin, R., Hiemstra, C., Zhong, Z., & Feijen, J. (2007). Enzyme-mediated fast *in situ* formation of hydrogels from dextran–tyramine conjugates. *Biomaterials*, *28*, 2791–2800.

Jin, R., Moreira Teixeira, L. S., Dijkstra, P. J., Zhong, Z., van Blitterswijk, C. A., Karperien, M., et al. (2010). Enzymatically crosslinked dextran–tyramine hydrogels as injectable scaffolds for cartilage tissue engineering. *Tissue Engineering, Part A*, *16*, 2429–2440.

Jin, R., Moreira Teixeira, L. S., Dijkstra, P. J., van Blitterswijk, C. A., Karperien, M., & Feijen, J. (2010). Enzymatically-crosslinked injectable hydrogels based on biomimetic dextran–hyaluronic acid conjugates for cartilage tissue engineering. *Biomaterials*, *31*, 3103–3113.

Jin, R., Moreira Teixeira, L. S., Dijkstra, P. J., van Blitterswijk, C. A., Karperien, M., & Feijen, J. (2011). Chondrogenesis in injectable enzymatically crosslinked heparin/dextran hydrogels. *Journal of Controlled Release*, *152*, 186–195.

Johnson, L. M., Fairbanks, B. D., Anseth, K. S., & Bowman, C. N. (2009). Enzyme-mediated redox initiation for hydrogel generation and cellular encapsulation. *Biomacromolecules*, *10*, 3114–3121.

Karaaslan, M. A., Tshabalala, M. A., Yelle, D. J., & Buschle-Diller, G. (2011). Nanoreinforced biocompatible hydrogels from wood hemicelluloses and cellulose whiskers. *Carbohydrate Polymers*, *86*, 192–201.

Kim, I. Y., Seo, S. J., Moon, H. S., Yoo, M. K., & Park, I. Y. (2008). Chitosan and its derivatives for tissue engineering applications. *Biotechnology Advances*, *26*, 1–21.

Kobayashi, S., Uyama, H., & Kimura, S. (2001). Enzymatic polymerization. *Chemical Reviews (Washington, DC, United States)*, *101*, 3793–3818.

Kretlow, J. D., Klouda, L., & Mikos, A. G. (2007). Injectable matrices and scaffolds for drug delivery in tissue engineering. *Advanced Drug Delivery Reviews*, *59*, 263–273.

Kurisawa, M., Chung, J. E., Yang, Y. Y., Gao, S. J., & Uyama, H. (2005). Injectable biodegradable hydrogels composed of hyaluronic acid-tyramine conjugates for drug delivery and tissue engineering. *Chemical Communications (Cambridge, United Kingdom)*, *34*, 4312–4314.

Lee, C. S. D., Gleghorn, J. P., Choi, N. W., Cabodi, M., Stroock, A. D., & Bonassar, L. J. (2007). Integration of layered chondrocytes-seeded alginate hydrogel scaffold. *Biomaterials*, *28*, 2987–2993.

Lee, F., Chung, J. E., & Kurisawa, M. (2008). An injectable enzymatically crosslinked hyaluronic acid–tyramine hydrogel system with independent tuning of mechanical strength and gelation rate. *Soft Matter*, *4*, 880–887.

Lee, F., Chung, J. E., & Kurisawa, M. J. (2009). An injectable hyaluronic acid-tyramine hydrogel system for protein delivery. *Journal of Controlled Release*, *134*, 186–193.

Lindblad, M. S., Albertsson, A.-C., Ranucci, E., Laus, M., & Giani, E. (2005). Biodegradable polymers from renewable sources: Rheological characterization of hemicellulose-based hydrogels. *Biomacromolecules*, *6*, 684–690.

Liu, Y., & Chan-Park, M. B. (2010). A biomimetic hydrogel based on methacrylated dextran-graft-lysine and gelatin for 3D smooth muscle cell culture. *Biomaterials*, *31*, 1158–1170.

Plunkett, M. L., & Hailey, J. A. (1990). An *in vivo* quantitative angiogénesis model using tumor cells entrapped in alginate. *Laboratory Investigation*, *62*, 510–517.

Polak, J. M., & Bishop, A. E. (2006). Stem cells and tissue engineering: Past, present, and future. *Annals of the New York Academy of Sciences*, *1068*, 352–366.

Sakai, S., Hirose, K., Taguchi, K., Ogushi, Y., & Kawakami, K. (2009). An injectable, *in situ* enzymatically gellable, gelatin derivative for drug delivery and tissue engineering. *Biomaterials*, *30*, 3371–3377.

Sperinde, J. J., & Griffith, L. G. (1997). Synthesis and characterization of enzymatically-cross-linked poly(ethylene glycol) hydrogels. *Macromolecules*, *30*, 5255–5264.

Stafford, R., Nyberg, S., Meier, S., White, J., Payne, W., Hu, W., et al. (1992). Hepatocyte function in a hollow fiber bioreactor: A potential bioartificial liver. *Journal of Surgical Research*, *53*, 549–557.

Sun, X.-F., Wang, H., Jing, Z., & Mohanathas, R. (2013). Hemicellulose-based pH-sensitive and biodegradable hydrogel for controlled drug delivery. *Carbohydrate Polymers*, *92*, 1357–1366.

Toledano, S., Williams, R. J., Jayawarna, V., & Ulijn, R. V. (2006). Enzyme-triggered self-assembly of peptide hydrogels via reversed hydrolysis. *Journal of the American Chemical Society*, *128*, 1070–1071.

Van Tomme, S. R., Storm, G., & Hennink, W. E. (2008). In situ gelling hydrogels for pharmaceutical and biomedical applications. *International Journal of Pharmaceutics*, *355*, 1–18.

Weng, L., Chen, X., & Chen, W. (2007). Rheological characterization of in situ crosslinkable hydrogels formulated from oxidized dextran and N-carboxyethyl chitosan. *Biomacromolecules*, *8*, 1109–1115.

Westhaus, E., & Messersmith, P. B. (2001). Triggered release of calcium from lipid vesiclesa bioinspired strategy for rapid gelation of polysaccharide and protein hydrogels. *Biomaterials*, *22*, 453–462.

Wichterle, O., & Lim, D. (1960). Hydrophilic gels for biological use. *Nature*, *185*, 117–118.

Xu, M., Wang, X., Yan, Y., Yao, R., & Ge, Y. (2010). An cell-assembly derived physiological 3D model of the metabolic syndrome, based on adipose-derived stromal cells and a gelatin/alginate/fibrinogen matrix. *Biomaterials*, *31*, 3868–3877.

Yang, J. Y., Zhou, X. S., & Fang, J. (2011). Synthesis and characterization of temperature sensitive hemicellulose-based hydrogels. *Carbohydrate Polymers*, *86*, 1113–1117.